HHS Public Access

Author manuscript

DNA Repair (Amst). Author manuscript; available in PMC 2021 February 18.

Published in final edited form as:

DNA Repair (Amst). 2020 June ; 90: 102861. doi:10.1016/j.dnarep.2020.102861.

Regulation of UV damage repair in quiescent yeast cells

Lindsey J. Long, **Po-Hsuen Lee**[#], **Eric M. Small**[#], **Cory Hillyer**[#], **Yan Guo**, **Mary Ann Osley**[*]

Molecular Genetics and Microbiology, University of New Mexico Health Sciences Center, Albuquerque, New Mexico USA 87131

Abstract

Non-growing quiescent cells face special challenges when repairing lesions produced by exogenous DNA damaging agents. These challenges include the global repression of transcription and translation and a compacted chromatin structure. We investigated how quiescent yeast cells regulated the repair of DNA lesions produced by UV irradiation. We found that UV lesions were excised and repaired in quiescent cells before their re-entry into S phase, and that lesion repair was correlated with high levels of Rad7, a recognition factor in the global genome repair sub-pathway of nucleotide excision repair (GGR-NER). UV exposure led to an increased frequency of mutations that included C->T transitions and T>A transversions. Mutagenesis was dependent on the error-prone translesion synthesis (TLS) DNA polymerase, Pol zeta, which was the only DNA polymerase present in detectable levels in quiescent cells. Across the genome of quiescent cells, UV-induced mutations showed an association with exons that contained H3K36 or H3K79 trimethylation but not with those bound by RNA polymerase II. Together, the data suggest that the distinct physiological state and chromatin structure of quiescent cells contribute toits regulation of UV damage repair.

Keywords

quiescent cells; UV mutagenesis; GGR-NER; Polymerase zeta

INTRODUCTION

Ultraviolet radiation produces DNA photoproducts that can have profound effects on cell survival. The presence of the bulky UV lesions, cyclobutane pyrimidine dimers (CPDs) and (6–4) pyrimidine-pyrimidone photoproducts (6–4 PPs), blocks progression of the DNA replication machinery during S phase [1, 2]. A specialized repair system, nucleotide excision repair (NER), recognizes the lesions and excises the DNA strand containing the lesion, allowing the replicative DNA polymerases to resume DNA synthesis [2]. Lesion recognition

[*]To whom correspondence should be addressed: Mary Ann Osley: Tel: +1-505-272-4839; Fax: +1- 505-272- 6029; mosley@salud.unm.edu.

[#]These authors made equal contributions

SUPPLEMENTARY DATA

Supplementary data include a Supplementary Figures pdf file with 10 figures, a Supplementary Figure Legends pdf file, and a Supplementary Tables 1–3 pdf file. Supplementary Table S4 is an Excel file.

CONFLICT OF INTEREST

None of the authors have any conflict of interests to report.

occurs through two sub-pathways of NER, the global genome repair (GGR) and transcription coupled repair (TCR) pathways, which employ different factors to initiate the repair cascade [3, 4]. Once the lesions are recognized, the pathways converge, with local DNA unwinding followed by endonucleolytic incision, removal of a single-stranded DNA oligonucleotide, repair synthesis to fill in the DNA gap, and finally, DNA end ligation. While NER is generally considered to be an error-free repair process, it also has a pro-mutagenic role after UV radiation [5]. Several mutagenic translesion synthesis (TLS) DNA polymerases can substitute for replicative DNA polymerases to directly bypass UV lesions by inserting an incorrect nucleotide opposite a lesion [6, 7]. Extension from a mis-paired base then results in mutations being fixed at lesion sites during the next round of DNA synthesis.

The stalling of DNA polymerases by UV lesions only occurs in cells that are actively replicating DNA. While the role of NER in removing or bypassing CPDs and 6–4 PPs during replication has been extensively studied, less is understood about how it repairs UV lesions in non-replicating cells. One important class of non-cycling cells are quiescent cells, which reside in G0 phase, a non-growing but viable state [8, 9]. All organisms have a quiescent state, and quiescence is an essential contributor to stem cell viability [8]. Importantly, quiescence is reversible, and in response to appropriate stimuli, cells resume growth, exit G0 and resume proliferation. Because quiescent cells are able to re-enter the cell cycle, how they respond to DNA damage is an important question, as the failure to accurately repair damaged DNA could result in the propagation of deleterious mutations to their progeny.

To investigate how NER regulates UV damage repair in non-replicating cells, we used a purified population of quiescent cells formed in budding yeast, *Saccharomyces cerevisiae*, which initiates quiescence when glucose is exhausted from the medium [9]. Following glucose exhaustion, cells enter stationary phase, at which point they can be physically separated into two distinct cell populations - a non-quiescent population that undergoes apoptosis and necrosis, and a quiescent population that has all the hallmarks of G0 phase cells, including global repression of transcription and translation, condensed chromatin structure, and the absence of DNA replication [10]. Importantly, the quiescent cell population remains viable, and when returned to glucose-containing medium, it resumes synthesis of key proteins, including those required for re-entry into the cell cycle. We used purified quiescent cells to examine their response to UV irradiation. UV irradiation led to the formation of CPD and 6–4PP photoproducts in these non-growing cells, and when the irradiated cells were transferred to glucose containing medium, the lesions were excised and repaired prior to the entry of these cells into S phase. This led to an elevated frequency of UV-induced mutations that included C>T transitions and T>A transversions. Lesion repair in these cells correlated with the presence of a key recognition factor in the GGR-NER pathway and increased levels of the TLS DNA polymerase, Pol zeta (Polζ). The data support the view that quiescent cells use a subset of NER factors to repair UV lesions, which may reflect the unique gene expression profiles and chromatin structure of these cells.

METHODS

Yeast strains and cell growth

Yeast strains are listed in Table S1. Strains were grown at 30°C in YPDA medium (1% yeast extract/2% peptone/2% glucose/0.04% adenine). Log phase cells were collected at OD_{600} = 0.8. Cells were arrested in the G1 phase of the cell cycle with alpha-factor [11], and quiescent cells were isolated by Percoll gradient centrifugation 7 days after culture inoculation (7Q cells) as previously described [10]. Cell size and morphology were assessed to ensure that purified populations of quiescent cells were isolated [10]. Cells were released from G1 arrest as previously described, and quiescent cells were washed and resuspended in pre-warmed YPD + 20 μg/ml nocodazole (NOCO) [11]. Because transcription and translation are globally repressed in quiescent cells, this step was necessary to initiate synthesis of key repair and replication factors following UV irradiation. The addition of nocodozole ensured that a single S phase was monitored.

Cell cycle analysis

The cell cycle progression of G1 or 7Q released cells was measured by counting the number of buds over time or by a modified flow cytometry protocol. Briefly, 0.4 OD_{600} units of cells were collected, resuspended in 0.5 ml of TE in the presence of 0.1 M Dithiothreitol (DTT), and incubated for 30 min at room temperature with gentle rotation. Cells were fixed in 70% ethanol overnight, washed once with 50 mM Tris-HCl (pH 8.0), and resuspended in 50 mM Tris with 1 mg/ml RNase A at 37°C overnight. Cells were collected by centrifugation, resuspended in 0.5 ml of pepsin solution (24 μl of concentrated HCl and 25 mg of pepsin in 5 ml of TE) and incubated at 37°C for 1 hr. Cell pellets were resuspended in 0.5 ml of PBS and sonicated for 10 sec. Another 0.5 ml of PBS with 0.2% NP-40 and 1 μM SYTOX-Green were added for 2 hr before running samples on a BD Biosciences FACS Calibur flow cytometer. Data acquisition (20,000 events) and analysis were performed with BD CellQuest™ software. Histograms were plotted, in which the y-axis represented the number of events and the x-axis represented the relative DNA content. Entry into S phase was also assessed by western blot analysis of Pol3-Myc levels after release of 7Q cells into YPD medium.

UV irradiation

The UV irradiation protocol was adapted from Dang duong Bang *et al.* [12]. Briefly, cells were collected and resuspended in cold, sterile PBS to OD_{600} units of 0.8. Fifteen ml of the cell suspension were transferred to a 10 cm Petri dish and irradiated with 254 nm UV light (Stratagene, Stratalinker 2400) at defined doses (J/m^2). After irradiation, cells were collected and immediately transferred to conical tubes wrapped in foil to prevent DNA damage repair by photolyases. For time course experiments, cells were resuspended at OD_{600} units of 0.8 in pre-warmed YPD and incubated in the dark at 30°C.

Spotting and viability assays

For spotting assays, cells were unirradiated or exposed to varying UV doses and diluted to 0.2 OD_{600} units in sterile water. Following 10-fold serial dilutions, 3 μl were spotted onto a

YPD (1% yeast extract, 2% peptone, 2% glucose) plate and incubated at 30°C in the dark for 1.5–2 days. For viability assays, UV irradiated cells were counted using a hemocytometer and plated in triplicate on YPD plates to yield approximately 50–300 colonies. Percent survival was calculated relative to colony numbers from a no-UV control culture after 2 days incubation in the dark at 30°C.

Canavanine reversion assay

Cells were unirradiated or exposed to various doses of UV to achieve similar survival among strains. Following UV exposure, cells were immediately spread in triplicate onto YPD plates to yield ~200 colonies per plate and ~1×10^8 cells were spread onto YPD + canavanine (60 μg/ml) plates. After 2–3 days growth at 30°C, the frequency of canavanine-resistant mutants (Can-r) was calculated relative to the total number of colonies on the YPD plates.

Measurement of CPD and 6–4 PP levels

Log phase, G1 arrested or 7Q cells were unirradiated or irradiated with 100 J/m^2 UV and immediately released into pre-warmed YPD medium. Before release and at intervals after release, 35 OD_{600} units of cells were collected, washed with 500 μL of sterile water, and resuspended in 300 μL of smash and grab buffer (2% Triton X-100, 1% SDS, 100 mM NaCl, 10 mM Tris, pH 8.0, 1mM EDTA, pH 8.0). After addition of 300 μL of phenol-chloroform-isoamyl alcohol (25:24:1; v/v) and 0.3 g of glass beads, samples were vortexed at highest speed at 4°C for 6 minutes, the supernatant was transferred to a new tube and the beads were washed with 200 μL of TE. The supernatants were combined and resuspended in 100 μL of TE. DNA concentration was measured by Nanodrop and ethidium bromide staining of ~2 μl of gDNA after 0.8% agarose gel electrophoresis.

Genomic DNA (gDNA) samples were diluted to a final volume of 50 μL in TE. Approximately 50, 100, and 200 ng of gDNA were used for measurement of the cellular levels of DNA, CPDs, and 6-4 PPs, respectively. Five μL of 4 M NaOH were added to each sample, followed by heating at 95°C for 5 minutes. Fifty μL of cold 2 M ammonium acetate (pH 7.0) were added, and the DNA samples were briefly centrifuged and stored on ice prior to loading onto a slot blot apparatus containing a nylon membrane (Bio-Rad, Zeta-Probe). After binding, the membrane was placed on chromatography paper (Fisher 05-714-4), soaked in denaturing solution (1.5 M NaCl, 0.5 M NaOH) for 10 minutes, and transferred to chromatography paper soaked in neutralization buffer (1.5 M NaCl, 0.5 M Tris, pH 7.0) for 5 minutes and then air dried. Membranes were incubated in blocking solution (0.75% milk/TBS-T (0.05% Tween) at room temperature for 1 hour and incubated with primary antibodies overnight. Anti-DNA (Millipore-Sigma, MAB3034) was used at 1:5000 in blocking solution at 4°C. Anti-CPD (GeneTex, GTX10347) and anti-6-4 PP (Cosmo-Bio, NMDND002, clone 64-M2) were used at 1:20000 in TBS-T (0.02% Tween) buffer at room temperature. Washing, secondary antibody incubation and visualization were performed as described for western blot analysis. Band densities were calculated with Image Studio software (LI-COR Biosciences).

Western blot analysis

All samples for western blot analysis were collected and processed for TCA lysates [13]. Lysates were separated by SDS-PAGE, transferred to an Immobilon-PVDF membrane, and incubated with primary antibodies overnight at 4°C. Lysate protein amounts and antibodies are listed in Table S2. After washing and incubation with secondary antibodies, bands on membranes were visualized by enhanced chemiluminescence (Bio-Rad; Clarity ECL Western kit) using X-Ray film.

Quantitative reverse transcription RNA analysis

Total RNA was extracted from log phase and 7Q cells [13], and qRT-PCR analysis was performed using the primers shown in Table S3.

Whole genome mutation analysis of UV irradiated 7Q cells

Three independent cultures of log phase cells were unirradiated and allowed to develop into quiescence, and 7Q cells were isolated by Percoll density gradient centrifugation. The 7Q cells were unirradiated or irradiated with 100 J/m^2 UV and plated onto YPD + canavanine plates. A single Can-r colony arising from each condition was inoculated into 20 mL of YPD and grown to an OD_{600} of ~ 4.0. Thirty OD_{600} units were collected and genomic DNA was extracted as described above, except that purified DNA was resuspended in 100 μL of nuclease-free water. DNA concentration was determined by Qubit fluorometric quantitation (Invitrogen, Qubit 2.0 Fluorimeter).

Genomic DNA was prepared for single-end DNA sequencing on an Illumina Nextseq 500 machine, using barcodes. DNA sequencing data were first trimmed by Trimmomatic [14], removing beginning and ending nucleotides with a base quality score less than 20 for each read. The trimmed data were aligned to *Saccharomyces cerevisiae* genome version sacCer3 (GCA_000146045.2) using BWA [15]. SNPs (single nucleotide polymorphisms) and indels (insertion/deletions) were called using Genome Analysis Tool Kit's Unified Genotyper. SNP and indel calls were quality controlled and filtered according to GATK's best practice. Gene annotations were conducted using ANNOVAR [16]. SNPs and indels that were common to either Log and 7Q minus UV samples were removed from further analysis. SNP signatures (defined as ref->alt allele frequency) were computed for each subtype of the samples and the mutation type was calculated. Up and downstream sequences that were 20 nucleotides from each SNP were extracted. The location of mutations on the transcribed or non-transcribed strand was determined by downloading coding strand DNA sequences as FASTA files that corresponded to those exomic regions annotated in the mutational spectra analysis (yeast strain S288C). The FASTA files were imported into UGENE 1.31.1, and the corresponding complementary strands were associated with the coding strands. The sequences adjacent to the mutation were identified using the UGENE search feature. The strand on which the mutation originated was then identified as either the non-transcribed or transcribed strand.

Statistical analyses

To test the null hypothesis that mutations occurred randomly in ORFs or intergenic regions, as well as on the transcribed or non-transcribed DNA strand, a two-tailed binomial test was performed. The theoretical distribution of ORFs was taken as 72.9% of the genome [17] and

the transcribed/non-transcribed strand ratio was assumed to be 50:50. To test the null hypothesis that mutated ORFs were randomly associated with RNAPII, H3K4me3, H3K36me3, or H3K79me3, a two-tailed Fisher's exact test was performed. A list of previously annotated ORFs enriched for RNAPII, H3K4me3, H3K36me3, or H3K79me3 in quiescent cells was obtained from Supplemental Table 2 in Young *et al.,* 2017 [13]. The Q and common ORF annotations from this table were combined as they define the total number of marked ORFs in quiescent cells. These annotated ORFs were then compared to ORFs containing mutations identified in the present study, to determine whether mutations fell in ORFs known to be associated with RNAPII, H3K4me3, H3K36me3, or H3K79me3 in quiescent cells. The null hypothesis was rejected when the P value was ≤ 0.05.

RESULTS

Quiescent cells are sensitive to UV irradiation and excise UV-induced lesions before their re-entry into S phase

Most DNA repair studies in nonproliferating cells have been performed with stationary phase cells, which are comprised of an approximately equal mix of quiescent and non-quiescent cells [10]. We used an established protocol to isolate quiescent yeast cells 7 days after culture inoculation (7Q) to examine the response of these cells to UV irradiation [13]. The ability to isolate a purified population of quiescent (Q) cells thus circumvented the undefined contributions of non-quiescent cells (NQ) present in a stationary phase culture to this analysis, as NQ cells exhibit considerable genome instability [10]. Quiescent cells were more sensitive to UV irradiation compared to proliferating cells (Log) or cells in the G1 phase of the cell cycle (Fig. 1A, B; Fig. S1A). These cells were also more sensitive than log cells after exposure to 4NQO (4-Nitroquinoline 1-oxide), a compound that reacts with DNA and mimics the effects of UV (Fig. S1B) [18]. After UV irradiation, both UV-induced cyclobutane pyrimidine dimers (CPDs) and (6–4) pyrimidine-pyrimidone photoproducts (6–4 PPs) were formed in quiescent cells at levels similar to those in log phase or G1 arrested cells (Fig. S2A, B). To determine the time frame in which these lesions were removed, 7Q cells were exposed to 100 J/m^2 UV and immediately released into fresh medium containing glucose to initiate growth and entry into the cell cycle. Because gene expression is globally repressed in quiescent cells, this step was necessary to promote the synthesis of all key repair and replication factors [13, 19]. The levels of CPDs and 6–4 PPs in genomic DNA were measured at various times after release. By 120 min after release, CPDs could no longer be detected in 7Q-irradiated cells (Fig. 2A, B). 6–4 PPs were also efficiently removed in quiescent cells during this same period, even faster than removal of CPDs (Fig. S3A, B). Thus, the sensitivity of quiescent cells to UV irradiation is not due to the presence of higher levels of UV lesions or the ability of these cells to remove DNA damage from the genome.

CPD and 6–4 PP lesions are repaired via the nucleotide excision repair (NER) pathway, and NER is required for repair of these lesions in both proliferating cells and in quiescent yeast cells [1, 20]. In replicating cells, these bulky lesions block the progression of replicative DNA polymerases [1]. During lesion repair in these cells, single-stranded DNA gaps are formed when DNA synthesis is re-initiated downstream of the lesions. The gaps activate an ATR/Mec1-dependent DNA checkpoint response that can be detected by phosphorylation of

the checkpoint kinase, Rad53 (Chk2), and histone H2A (pH2A) [1, 21, 22]. Once the gap has been filled in, the checkpoint is relieved and replication resumes. UV irradiation also induces phosphorylation of checkpoint proteins in noncycling human cells through the ATR kinase [23, 24]. To investigate if a checkpoint response was triggered in UV irradiated quiescent yeast cells, samples were collected for western blot analysis following exposure of cells to 100 J/m^2 of UV and at various times after their release into glucose-containing medium. Both Rad53 and H2A were phosphorylated 30 minutes after irradiation, and phosphorylation was removed from both proteins by 120 min (Fig. 2C). To confirm that the checkpoint was active in quiescent cells and not in cells that had re-entered the cell cycle, we measured the time at which DNA synthesis was initiated after release of the UV irradiated quiescent cells into growth medium (Fig. S4). These cells did not initiate DNA replication until ~180 minutes after their release into glucose-containing medium, indicating that the checkpoint response was resolved in non-cycling cells. Moreover, the co-incident timing of UV lesion removal and resolution of the UV-induced checkpoint was also consistent with repair occurring in quiescent cells before their entry into S phase. These data support genetic studies showing that UV-induced mutations are fixed on both DNA strands in nonproliferating quiescent cells prior to the initiation of DNA replication [20].

Quiescent cells contain a subset of NER factors that recognize UV-induced lesions

The NER pathway is divided into two sub-pathways that differ by the recognition of UV-induced lesions in DNA before they converge at the step of DNA opening and lesion incision [2, 3]. In the transcription-coupled TCR-NER pathway, elongating RNA polymerase II (RNAP II) is blocked when it encounters a lesion in the transcribed strand of active genes, and it then recruits the ATPase, Rad26, to initiate repair [4]. In the global genome-repair GGR-NER pathway, DNA lesions are scanned for in both transcribed and non-transcribed DNA strands of active and inactive genes and are bound by the factors Rad16 and Rad7 [25–28]. We focused on key TCR-NER and GGR-NER recognition factors in proliferating cells, during the development of quiescent cells, and in purified quiescent cells, to determineif there was a difference in their expression. *RAD7* (GGR), *RAD1*6 (GGR), and *RAD2*6 (TCR) RNAs were present in quiescent cells at levels similar to or higher than those seen in proliferating cells (Fig. 3A; Fig. S8). However, when the levels of Rad7 (GGR) and Rad26 (TCR) proteins were examined, the Rad7 protein was detected at higher levels in quiescent cells compared to log cells (Fig. 3B). The Rad26 protein was present in proliferating cells but disappeared during the development of quiescent cells, and conversely, the Rad7 protein was present at very low levels in log phase cells but accumulated during Q cell development (Fig. 3B). Additionally, after UV irradiated quiescent cells were released into the cell cycle, Rad7 protein remained at high levels both during and after the period of gap repair (Fig. S9).

These data suggested that the transcription-independent GGR-NER pathway might play an important role in signaling the repair of UV-induced lesions in quiescent cells, which is supported by the global shut-down of transcription in these cells [19]. To address this, we measured the effect of deleting the *RAD7*, *RAD16*, or *RAD26* genes on the frequency of canavanine-resistant (Can-r) mutations in quiescent cells after their exposure to UV [29]. WT 7Q cells had a higher frequency of UV-induced Can-r mutations than either proliferating cells (32-fold) or nonreplicating G1 arrested cells (~9-fold), while little to no difference was

observed in the frequency of spontaneous Can-r mutations among the three cell types (Fig. 4; Fig S5). Thus, UV-induced lesions in non-replicating quiescent cells are repaired via a pro-mutagenic pathway, as has previously been reported [5, 20]. Compared to the levels seen in WT cells, UV-induced Can-r mutations in *rad7*Δ and *rad16*Δ cells were reduced ~5–8-fold, while no change in mutation frequency was seen in a *rad26*Δ strain (Fig. 5A). In addition to Rad26, the RNAP subunit, Rpb9, also contributes to TCR-NER through its role in transcription elongation [30, 31]. However, quiescent cells did not form in a *rad26*Δ *rpb9*Δ double mutant, so we were unable to test its contribution to this pathway. Moreover, while CPDs were formed in both *rad7*Δ and *rad26*Δ quiescent cells (Fig. S2C), their removal was almost completely impaired in a *rad7*Δ mutant, but not in a *rad26*Δ mutant, consistent with a defect in lesion recognition by the GGR-NER pathway (Fig. S6A, B). This is supported by the increased UV sensitivity of *rad7*Δ or *rad16*Δ quiescent cells compared to *rad26*Δ quiescent cells (Fig. S7A). Together with the effects of *rad7*Δ and *rad16*Δ mutations on *CAN* mutagenesis and CPD removal, the data support the conclusion that the activity of the GGR-NER pathway contributes a significant role to the recognition of UV lesions and their subsequent repair in quiescent cells. As discussed later, these results are in contrast to a report that the TCR-NER pathway is required for mutagenesis in quiescent yeast cells isolated by a different method [20].

DNA polymerase zeta is present in quiescent cells

Error-prone translesion synthesis (TLS) DNA polymerases play important cellular functions by substituting for error-free replicative polymerases to bypass blocking DNA lesions that remain during DNA replication [32, 33]. These polymerases overcome the block by inserting an incorrect base opposite a lesion, thereby generating mutations upon the next round of replication [6, 7, 33]. The TLS DNA polymerases, Pol eta (Polη), Pol zeta (Polζ) and the Polζ-associated factor, Rev1, contribute to lesion bypass in yeast, and Polζ is responsible for the majority of spontaneous and UV-induced mutations in this organism [32, 34, 35]. We first asked whether there was a difference in the expression of TLS DNA polymerases between proliferating and quiescent cells. The levels of RNAs from genes encoding the catalytic subunits of the three replicative polymerases, *POL1* (Pol alpha/Polα), *POL2* (Pol epsilon/Polε) and *POL3* (Pol delta/Polδ), were reduced in quiescent cells compared to proliferating cells, consistent with the expression of these genes in S phase (Fig. 3A; Fig. S8). The proteins corresponding to all three of these polymerase subunits were also present in proliferating cells, but their levels significantly decreased during the development of quiescent cells, correlating with the absence of DNA synthesis in these G0 cells (Fig. 3C). Similarly, Rad30, the Polη catalytic subunit, and Rev1, a Polζ associated protein, were also present in growing cells but decreased to very low levels in quiescent cells, although the RNAs encoded by these genes were detected in both cell types (Fig. 3A, C; Fig. S8). In striking contrast, Rev3, the catalytic subunit of Polζ, was almost undetectable in proliferating cells but accumulated in cells as quiescence developed. Among the six DNA polymerases, only Rev3 was present at high levels in quiescent cells (Fig. 3C), and its levels remained high during the period of gap repair after UV irradiated quiescent cells were released into the cell cycle (Fig S9).

We next asked if the levels of the TLS polymerases in quiescent cells showed a correlation with the repair of UV-induced CPD lesions and *CAN*1 mutagenesis. CPD lesions were formed and efficiently removed in quiescent cells in the absence of either *RAD30* or *REV3* (Fig. S2D; Fig. S6A, C). However, UV-induced Can-r mutations in 7Q cells were almost completely eliminated in *rev3*Δ and *rev1*Δ cells, but not in *rad30*Δ cells (Fig. 5B). This is consistent with genetic evidence showing that Polζ is required for the generation of suppressor mutations in the adenine biosynthetic pathway in quiescent cells and for the increased levels of mutagenesis characteristic of aging quiescent cells [20, 36, 37]. Together, the data provide strong supporting evidence that the unique presence of Polζ in quiescent cells accounts for the dependence of these cells on this TLS polymerase for UV-induced mutagenesis.

UV-induced mutation spectra in quiescent cells

In contrast to proliferating cells, quiescent cell chromatin is deacetylated and transcription is globally repressed [13, 19]. We asked if the UV-induced mutation spectra of quiescent cells reflected these features of the Q cell epigenome by exposing three independently isolated populations of 7Q cells to 100 J/m^2 UV, followed by whole genome DNA sequencing. To identify mutations that were specific to UV irradiated quiescent cells, we eliminated mutations present in log phase cells prior to their development into quiescent cells and in 7Q cells that had not been exposed to UV. This resulted in a total of 76 unique mutations from the combined data, with single nucleotide insertions comprising the most frequent class of UV-induced Q cell mutations and indels making up a very small fraction of the total (Table S4). The highest percentage of mutations included CG->TA (C>T) and TA->CG (T>C) transitions, and also a class of TA->AT transversions (T>A) (Fig 6A; Fig. S10). C>T and T>C mutations occurred most frequently in the context of pyrimidine-pyrimidine bases, while T>A mutations occurred in a TA-rich context (Table S4; Fig. S10).

We next asked if the mutations in quiescent cells were present in specific chromosomal regions or in regions with distinct chromatin features. Approximately 73% of the yeast genome is present in exons [17]. However, mutations were not significantly enriched in exons in 7Q cells as they were similarly distributed relative to the entire genome (Materials and Methods; Table S4; p=0.194). Additionally, mutations were present on both transcribed and non-transcribed strands without a significant bias (Materials and Methods; Table S4; p=0.155) and were not significantly associated with exons that were occupied by RNA polymerase II (RNAP II) (Fig. 6B). Together, these data further support a role for the transcription-independent GGR-NER pathway in the repair of UV lesions in quiescent cells. The chromatin of quiescent cells is deacetylated but retains three marks of histone methylation (H3K4me3, H3K36me3, H3K79me3) that are usually associated with active transcription [13]. We have reported that these marks were most likely laid down in chromatin prior to or during the development of quiescent cells and then retained in these cells after transcription was repressed [13]. Interestingly, a significant number of 7Q mutations fell in exons marked with H3K36 or H3K79 trimethylation (Figure 6B). Finally, following UV exposure and release of quiescent cells into the cell cycle, acetylation of H3 lysine 9 and lysine 14 (H3K9ac/K14ac) occurred rapidly and was restored during the period of gap repair (Fig. S9). These latter modifications are associated with open chromatin and

have been linked to chromatin remodeling during GGR-NER [38–40]. Thus, the presence of these various H3 modifications might promote a chromatin structure in quiescent cells that is more accessible to repair by the GGR-NER pathway.

DISCUSSION

In this study, we used a combination of genetic, molecular and genomic approaches to investigate the regulation of UV-induced DNA damage repair in a pure population of quiescent yeast cells. The results support the view that UV lesions were formed at similar levels in proliferating and quiescent cells and excised and repaired in quiescent cells after they resumed growth but before they entered S phase. UV repair in quiescent cells correlated with the presence of a key lesion recognition factor in the global genome repair NER pathway and the absence of a similar factor in the transcription-coupled NER pathway. The UV sensitivity of quiescent cells was accompanied by an increased frequency of mutations that was dependent on the error-prone translesion DNA polymerase, Polζ, the only DNA polymerase present at detectable levels in these cells. Across the genome of quiescent cells, mutations were distributed between exons and intergenic regions without a bias, and exons that contained mutations were not associated with RNAPII but were marked with H3K36 and H3K79 trimethylation. Together, the data support the view that quiescent cells have a distinct physiological and chromatin environment that contributes to UV-induced mutagenesis.

An extensive genetic analysis of NER mutants has provided evidence that UV-induced suppressor mutations in the adenine biosynthetic pathway arise in quiescent cells prior to their entry into S phase [20]. In the present study, we obtained additional data to support the conclusion that UV lesions are repaired in quiescent cells before they re-enter S phase. First, UV-induced CPD and 6–4 PP lesions were removed from the genome of quiescent cells before these cells initiated DNA replication. Second, UV irradiation induced a checkpoint response in quiescent cells that was consistent with the formation of single-stranded DNA gaps, and the checkpoint was resolved before the initiation of S phase. Together, the co-incident timing of CPD removal and inactivation of the UV-induced checkpoint support the view that gap repair occurred in non-replicating quiescent cells.

Molecular, genetic, and genomic data indicated that the transcription-independent global genome repair (GGR) sub-pathway of NER plays an important role in UV lesion repair in quiescent cells. First, Rad7, a GGR factor that recognizes UV lesions, was present in quiescent cells at much higher levels than in growing cells, and its levels remained high in UV exposed quiescent cells both during and after the period of gap repair. In contrast, the RNAP II-associated TCR recognition factor, Rad26, disappeared during the development of quiescence and was not detected in quiescent cells. Second, it has been shown that transcription is globally repressed in quiescent cells, with the active forms of RNAP II present at very low levels in these cells [13, 19]. Moreover, UV mutations were localized in exons that were not significantly associated with RNAP II and were randomly distributed between transcribed and non-transcribed DNA strands [28, 31]. Third, the frequency of Can-r mutations was lower in *rad7*Δ and *rad16*Δ GGR mutants compared to a wild type strain or a *rad26*Δ TCR mutant. These combined data support the conclusion that the recognition of

UV lesions in quiescent cells primarily occurs via the GGR-NER pathway, which can act on both expressed and non-expressed genes [27, 28, 41]. However, in contrast to the decrease in Can-r mutations in a *rev3*Δ mutant, which has a defect in the catalytic subunit of the Polζ TLS DNA polymerase, Can-r mutations were not completely eliminated in either a *rad7*Δ or *rad16*Δ mutant. This suggests that another repair pathway operates in quiescent cells when the global genome repair pathway is defective. A previous study, using another method to isolate quiescent cells, reported a dependency on the transcription-coupled NER pathway to initiate suppressor mutations in the adenine biosynthetic pathway in quiescent cells exposed to UV [20]. It is therefore possible that in the absence of GGR-NER, a subset of Can-r mutations arose via combined Rad26-dependent initiation of TCR-NER and residual low-level activity of transcribing RNA polymerase II. We could not directly test this possibility, as a *rad26*Δ *rpb9*Δ double mutant, in which TCR-NER is eliminated, did not form quiescent cells in our system.

Genetic studies have found that UV induced mutagenesis in quiescent yeast cells is dependent on the error-prone TLS DNA polymerase, Polζ [20]. We found a similar genetic dependency on Polζ using a forward assay for canavanine-resistant mutations [29], confirming the important role of this TLS polymerase in mutagenesis in these non-growing cells. Importantly, the Rev3 protein, the catalytic subunit of Polζ, was the only DNA polymerase present at high levels in quiescent cells and during the period of gap repair. In striking contrast, the replicative DNA polymerases and a second TLS DNA polymerase, Polη, were present in proliferating cells but their levels dropped sharply as quiescent cells developed. Together, the data support the view that UV-induced mutagenesis in quiescent cells results because only Polζ is present to fill gaps created by NER in these cells. The activity of this mutagenic DNA polymerase may also account for the decreased viability of quiescent cells following their exposure to UV.

Polζ is responsible for most UV-induced mutations in proliferating yeast cells through its role in the bypass of UV blocking lesions during DNA replication [1]. It has been proposed that the primary role of Polζ is to extend DNA from a mis-matched base pair after a second TLS polymerase such as Polη inserts an incorrect nucleotide opposite a UV lesion [42]. However, it has also been reported that in the absence of Polη, Polζ itself can directly bypass a UV lesion with low efficiency both *in vitro* and *in vivo* [43–45]. As a result of this activity, Polζ mis-inserts nucleotides opposite dipyrimidine CC or TT dimers, leading to C>T, T>C, and T>A mutations [43]. These mutations represented the most frequent classes of mutations found in the genome of UV irradiated quiescent cells, thereby providing additional evidence that Polζ on its own bypasses UV lesions and promotes mutagenesis in non-growing cells. Interestingly, these mutational signatures are similar to a recently identified “split” signature of the UV associated SBS7 signature in human skin cancer cells, in which T>C and T>A mutations have been identified at lower frequencies than the more abundant C>T mutations [46]. By analogy to the results in quiescent yeast cells, it is possible that these constituent signatures might represent error-prone repair of UV damage by Polζ in quiescent populations of skin cells.

How is Polζ recruited to UV lesion sites in quiescent cells? In proliferating cells TLS polymerases are recruited to replication-blocking UV lesions via interactions with PCNA.

The Rev1 protein acts as a bridge to bring Polζ to these sites through its interactions with both PCNA and Rev7, the stimulatory subunit of Polζ [47–50]. However, consistent with the absence of DNA synthesis in quiescent cells, PCNA transcript levels were very low in these cells. Rev1 protein levels were also lower in quiescent cells than in proliferating cells, but these levels may be sufficient to recruit Polζ to lesion sites, perhaps through the ability of Rev1 to bind to ssDNA gaps and primer termini rather than to PCNA [51, 52].

Chromatin structure has a profound influence on the repair of UV lesions by restricting access of the NER machinery to sites of DNA damage [53–55]. While the genome of quiescent cells is present in condensed, deacetylated chromatin, exons that contained mutations were marked with H3K36 or H3K79 trimethylation. These marks have been postulated to be laid down and then retained on chromatin during the development of quiescent cells, and thus do not represent the presence of actively transcribed chromatin in these cells [13]. However, the presence of these modifications may generally alter chromatin structure to allow access of NER repair factors. Alternatively, H3K79 methylation itself may be important during NER in quiescent cells. In proliferating cells, Dot1 mediated H3K79 methylation has been reported to play a key role in promoting NER by the GGR-NER pathway, which appears to be an important NER pathway in quiescent cells [56, 57]. It has been suggested that this histone modification could act as a docking site for the GGR machinery on chromatin, although this has not yet been firmly established. In addition, the low levels of histone Gcn5-dependent H3K9 and K14 acetylation in quiescent cells were rapidly restored when quiescent cells re-entered the cell cycle. These modifications have also been linked to the facilitation of GGR-NER through recruitment of nucleosome remodeling activities [38, 39]. Taken together, the data suggest that the distinctive chromatin structure of quiescent cells could play an important role in promoting access of NER factors to sites of UV lesions.

CONCLUSIONS

In summary, quiescent cells contain a subset of NER factors that initiate and repair UV induced DNA damage during their return to growth and before these cells re-enter S phase. UV lesion repair is associated with high levels of the GGR-NER recognition factor, Rad7, and the mutagenic translesion DNA polymerase, Polζ, in these cells. Quiescent cells have elevated numbers of UV-induced mutations that occur in exons that are not highly associated with RNA polymerase II but have retained H3K46 or H3K79 methylation. Thus, the response of quiescent cells to UV damage appears to be mediated by the unique physiological and epigenetic environment of these cells.

Supplementary Material

Refer to Web version on PubMed Central for supplementary material.

ACKNOWLEDGEMENTS

Peng Mao, Alan Tomkinson, and Mark McCormick are thanked for helpful comments and advice. The Analytical and Translational Genomics and Bioinformatics Shared Resources of the UNM Comprehensive Cancer Center provided expert technical support.

FUNDING

This work was supported by the National Institutes of Health, National Institute of Aging (AG054494 to M.A.O); National Institutes of Health, National Cancer Institute (P30 CA118100 to Cheryl Willman); and National Institutes of Health, General Medical Sciences (K12 GM088021 to Angela Wandinger-Ness). Funding for open access charge-National Institutes of Health.

REFERENCES

1. Novarina D, et al., Mind the gap: keeping UV lesions in check. DNA Repair (Amst), 2011 10(7): p. 751–9. [PubMed: 21602108]
2. Scharer OD, Nucleotide excision repair in eukaryotes. Cold Spring Harb Perspect Biol, 2013 5(10): p. a012609. [PubMed: 24086042]
3. Petruseva IO, Evdokimov AN, and Lavrik OI, Molecular mechanism of global genome nucleotide excision repair. Acta Naturae, 2014 6(1): p. 23–34. [PubMed: 24772324]
4. Sarasin A and Stary A, New insights for understanding the transcription-coupled repair pathway. DNA Repair (Amst), 2007 6(2): p. 265–9. [PubMed: 17194629]
5. Heidenreich E, et al., A mutation-promotive role of nucleotide excision repair in cell cycle-arrested cell populations following UV irradiation. DNA Repair (Amst), 2010 9(1): p. 96–100. [PubMed: 19910266]
6. Sale JE, Translesion DNA synthesis and mutagenesis in eukaryotes. Cold Spring Harb Perspect Biol, 2013 5(3): p. a012708. [PubMed: 23457261]
7. Waters LS, et al., Eukaryotic translesion polymerases and their roles and regulation in DNA damage tolerance. Microbiol Mol Biol Rev, 2009 73(1): p. 134–54. [PubMed: 19258535]
8. Cheung TH and Rando TA, Molecular regulation of stem cell quiescence. Nat Rev Mol Cell Biol, 2013 14(6): p. 329–40. [PubMed: 23698583]
9. De Virgilio C, The essence of yeast quiescence. FEMS Microbiol Rev, 2012 36(2): p. 306–39. [PubMed: 21658086]
10. Allen C, et al., Isolation of quiescent and nonquiescent cells from yeast stationary-phase cultures. J Cell Biol, 2006 174(1): p. 89–100. [PubMed: 16818721]
11. Trujillo KM and Osley MA, A role for H2B ubiquitylation in DNA replication. Mol Cell, 2012 48(5): p. 734–46. [PubMed: 23103252]
12. Bang DD, et al., Regulation of the Saccharomyces cerevisiae DNA repair gene RAD16. Nucleic Acids Res, 1995 23(10): p. 1679–85. [PubMed: 7784171]
13. Young CP, et al., Distinct histone methylation and transcription profiles are established during the development of cellular quiescence in yeast. BMC Genomics, 2017 18(1): p. 107. [PubMed: 28122508]
14. Bolger AM, Lohse M, and Usadel B, Trimmomatic: a flexible trimmer for Illumina sequence data. Bioinformatics, 2014 30(15): p. 2114–20. [PubMed: 24695404]
15. Li H and Durbin R, Fast and accurate short read alignment with Burrows-Wheeler transform. Bioinformatics, 2009 25(14): p. 1754–60. [PubMed: 19451168]
16. Wang K, Li M, and Hakonarson H, ANNOVAR: functional annotation of genetic variants from high-throughput sequencing data. Nucleic Acids Res, 2010 38(16): p. e164. [PubMed: 20601685]
17. Alexander RP, et al., Annotating non-coding regions of the genome. Nat Rev Genet, 2010 11(8): p. 559–71. [PubMed: 20628352]
18. Downes DJ, et al., Characterization of the mutagenic spectrum of 4-nitroquinoline 1-oxide (4-NQO) in Aspergillus nidulans by whole genome sequencing. G3 (Bethesda), 2014 4(12): p. 2483–92. [PubMed: 25352541]
19. McKnight JN, et al., Global Promoter Targeting of a Conserved Lysine Deacetylase for Transcriptional Shutoff during Quiescence Entry. Mol Cell, 2015 59(5): p. 732–43. [PubMed: 26300265]
20. Kozmin SG and Jinks-Robertson S, The mechanism of nucleotide excision repair-mediated UV-induced mutagenesis in nonproliferating cells. Genetics, 2013 193(3): p. 803–17. [PubMed: 23307894]

21. Matsumoto M, et al., Perturbed gap-filling synthesis in nucleotide excision repair causes histone H2AX phosphorylation in human quiescent cells. J Cell Sci, 2007 120(Pt 6): p. 1104–12. [PubMed: 17327276]
22. Giannattasio M, et al., Physical and functional interactions between nucleotide excision repair and DNA damage checkpoint. EMBO J, 2004 23(2): p. 429–38. [PubMed: 14726955]
23. Vrouwe MG, et al., UV-induced photolesions elicit ATR-kinase-dependent signaling in non-cycling cells through nucleotide excision repair-dependent and -independent pathways. J Cell Sci, 2011 124(Pt 3): p. 435–46. [PubMed: 21224401]
24. Shaj K, Hutcherson RJ, and Kemp MG, ATR Kinase Activity Limits Mutagenesis and Promotes the Clonogenic Survival of Quiescent Human Keratinocytes Exposed to UVB Radiation. Photochem Photobiol, 2019.
25. Guzder SN, et al., Yeast Rad7-Rad16 complex, specific for the nucleotide excision repair of the nontranscribed DNA strand, is an ATP-dependent DNA damage sensor. J Biol Chem, 1997 272(35): p. 21665–8. [PubMed: 9268290]
26. Reed SH, You Z, and Friedberg EC, The yeast RAD7 and RAD16 genes are required for postincision events during nucleotide excision repair. In vitro and in vivo studies with rad7 and rad16 mutants and purification of a Rad7/Rad16-containing protein complex. J Biol Chem, 1998 273(45): p. 29481–8. [PubMed: 9792654]
27. Wang Z, et al., The RAD7, RAD16, and RAD23 genes of Saccharomyces cerevisiae: requirement for transcription-independent nucleotide excision repair in vitro and interactions between the gene products. Mol Cell Biol, 1997 17(2): p. 635–43. [PubMed: 9001217]
28. Li S, et al., The roles of Rad16 and Rad26 in repairing repressed and actively transcribed genes in yeast. DNA Repair (Amst), 2007 6(11): p. 1596–606. [PubMed: 17611170]
29. Gocke E and Manney TR, Expression of radiation-induced mutations at the arginine permease (CAN1) locus in Saccharomyces cerevisiae. Genetics, 1979 91(1): p. 53–66. [PubMed: 372046]
30. Li S, et al., Modulation of Rad26- and Rpb9-mediated DNA repair by different promoter elements. J Biol Chem, 2006 281(48): p. 36643–51. [PubMed: 17023424]
31. Li S and Smerdon MJ, Dissecting transcription-coupled and global genomic repair in the chromatin of yeast GAL1–10 genes. J Biol Chem, 2004 279(14): p. 14418–26. [PubMed: 14734564]
32. Goodman MF and Woodgate R, Translesion DNA polymerases. Cold Spring Harb Perspect Biol, 2013 5(10): p. a010363. [PubMed: 23838442]
33. Prakash S, Johnson RE, and Prakash L, Eukaryotic translesion synthesis DNA polymerases: specificity of structure and function. Annu Rev Biochem, 2005 74: p. 317–53. [PubMed: 15952890]
34. Makarova AV and Burgers PM, Eukaryotic DNA polymerase zeta. DNA Repair (Amst), 2015 29: p. 47–55. [PubMed: 25737057]
35. Northam MR, et al., Participation of DNA polymerase zeta in replication of undamaged DNA in Saccharomyces cerevisiae. Genetics, 2010 184(1): p. 27–42. [PubMed: 19841096]
36. Madia F, et al., Oncogene homologue Sch9 promotes age-dependent mutations by a superoxide and Rev1/Polζeta-dependent mechanism. J Cell Biol, 2009 186(4): p. 509–23. [PubMed: 19687253]
37. Gangloff S and Arcangioli B, DNA repair and mutations during quiescence in yeast. FEMS Yeast Res, 2017 17(1).
38. Yu Y, et al., UV irradiation stimulates histone acetylation and chromatin remodeling at a repressed yeast locus. Proc Natl Acad Sci U S A, 2005 102(24): p. 8650–5. [PubMed: 15939881]
39. Waters R, van Eijk P, and Reed S, Histone modification and chromatin remodeling during NER. DNA Repair (Amst), 2015 36: p. 105–13. [PubMed: 26422133]
40. Yu S, et al., How chromatin is remodelled during DNA repair of UV-induced DNA damage in Saccharomyces cerevisiae. PLoS Genet, 2011 7(6): p. e1002124. [PubMed: 21698136]
41. Scott AD and Waters R, The Saccharomyces cerevisiae RAD7 and RAD16 genes are required for inducible excision of endonuclease III sensitive-sites, yet are not needed for the repair of these lesions following a single UV dose. Mutat Res, 1997 383(1): p. 39–48. [PubMed: 9042418]
42. Guo D, et al., Translesion synthesis by yeast DNA polymerase zeta from templates containing lesions of ultraviolet radiation and acetylaminofluorene. Nucleic Acids Res, 2001 29(13): p. 2875–83. [PubMed: 11433034]

43. Stone JE, et al., Lesion bypass by S. cerevisiae Pol zeta alone. DNA Repair (Amst), 2011 10(8): p. 826–34. [PubMed: 21622032]
44. Zhong X, et al., The fidelity of DNA synthesis by yeast DNA polymerase zeta alone and with accessory proteins. Nucleic Acids Res, 2006 34(17): p. 4731–42. [PubMed: 16971464]
45. Gibbs PE, et al., The relative roles in vivo of Saccharomyces cerevisiae Pol eta, Pol zeta, Rev1 protein and Pol32 in the bypass and mutation induction of an abasic site, T-T (6–4) photoadduct and T-T cis-syn cyclobutane dimer. Genetics, 2005 169(2): p. 575–82. [PubMed: 15520252]
46. Alexandrov LB, et al., Signatures of mutational processes in human cancer. Nature, 2013 500(7463): p. 415–21. [PubMed: 23945592]
47. Acharya N, et al., Complex formation with Rev1 enhances the proficiency of Saccharomyces cerevisiae DNA polymerase zeta for mismatch extension and for extension opposite from DNA lesions. Mol Cell Biol, 2006 26(24): p. 9555–63. [PubMed: 17030609]
48. Heidenreich E, Eisler H, and Steinboeck F, Epistatic participation of REV1 and REV3 in the formation of UV-induced frameshift mutations in cell cycle-arrested yeast cells. Mutat Res, 2006 593(1–2): p. 187–95. [PubMed: 16154164]
49. Lawrence CW, Cellular roles of DNA polymerase zeta and Rev1 protein. DNA Repair (Amst), 2002 1(6): p. 425–35. [PubMed: 12509231]
50. Waters LS and Walker GC, The critical mutagenic translesion DNA polymerase Rev1 is highly expressed during G(2)/M phase rather than S phase. Proc Natl Acad Sci U S A, 2006 103(24): p. 8971–6. [PubMed: 16751278]
51. de Groote FH, et al., The Rev1 translesion synthesis polymerase has multiple distinct DNA binding modes. DNA Repair (Amst), 2011 10(9): p. 915–25. [PubMed: 21752727]
52. Masuda Y and Kamiya K, Role of single-stranded DNA in targeting REV1 to primer termini. J Biol Chem, 2006 281(34): p. 24314–21. [PubMed: 16803901]
53. Dinant C, Houtsmuller AB, and Vermeulen W, Chromatin structure and DNA damage repair. Epigenetics Chromatin, 2008 1(1): p. 9. [PubMed: 19014481]
54. Li S, Implication of posttranslational histone modifications in nucleotide excision repair. Int J Mol Sci, 2012 13(10): p. 12461–86. [PubMed: 23202908]
55. Reed SH, Nucleotide excision repair in chromatin: damage removal at the drop of a HAT. DNA Repair (Amst), 2011 10(7): p. 734–42. [PubMed: 21600858]
56. Chaudhuri S, Wyrick JJ, and Smerdon MJ, Histone H3 Lys79 methylation is required for efficient nucleotide excision repair in a silenced locus of Saccharomyces cerevisiae. Nucleic Acids Res, 2009 37(5): p. 1690–700. [PubMed: 19155276]
57. Tatum D and Li S, Evidence that the histone methyltransferase Dot1 mediates global genomic repair by methylating histone H3 on lysine 79. J Biol Chem, 2011 286(20): p. 17530–5. [PubMed: 21460225]

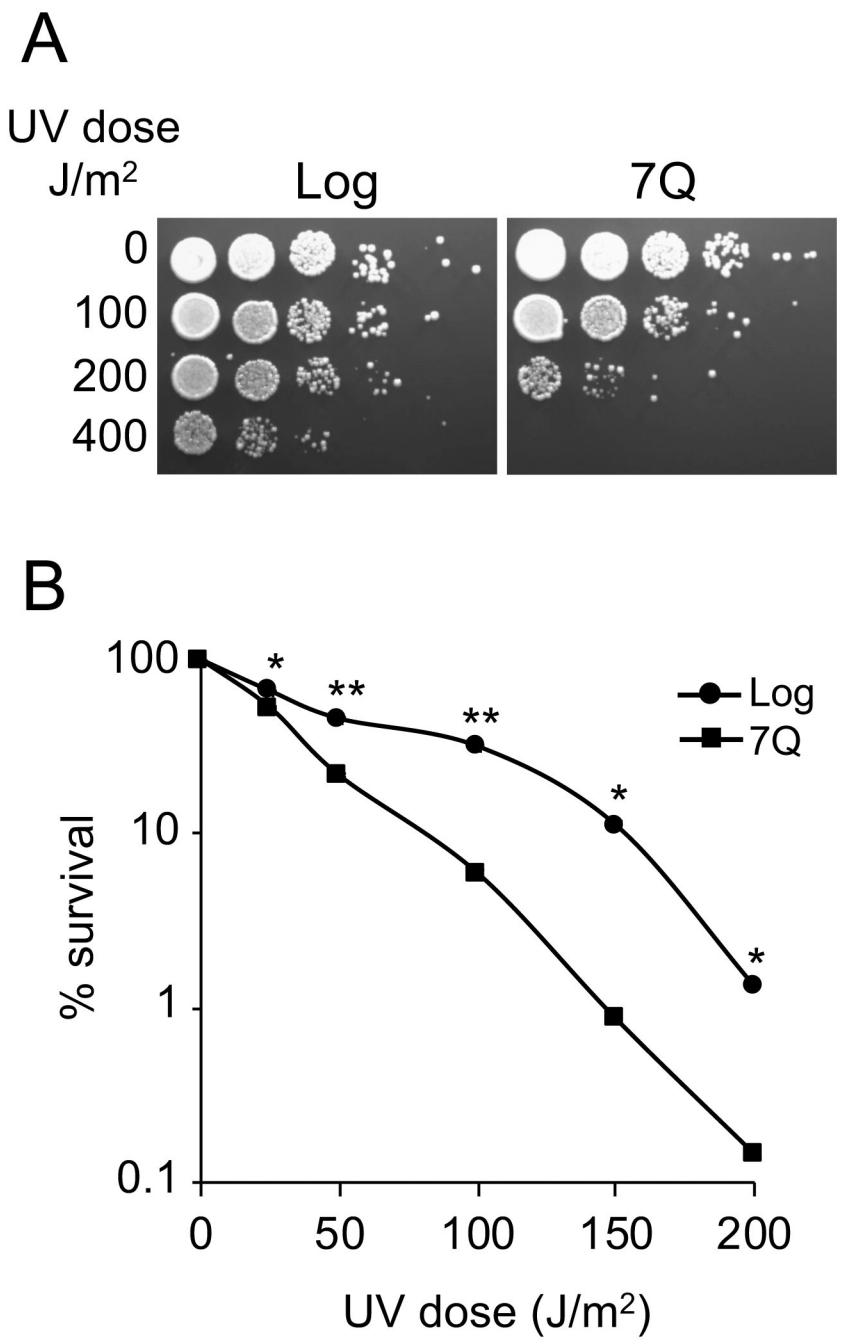

Figure 1. Quiescent cells are sensitive to UV irradiation.

Exponentially growing (Log) and quiescent cells (7Q) were irradiated with various doses of UVC.

A. 10-fold serial dilutions were spotted onto YPD plates and incubated for 2 days at 30°C.

B. Cells were plated in triplicate onto YPD plates. Percent survival was calculated relative to survival of Log or 7Q cells in the absence of UV, and represents the average of 3–5 independent experiments with standard deviation. P values <0.05 (*) or <0.01 (**) as determined by Student's T test.

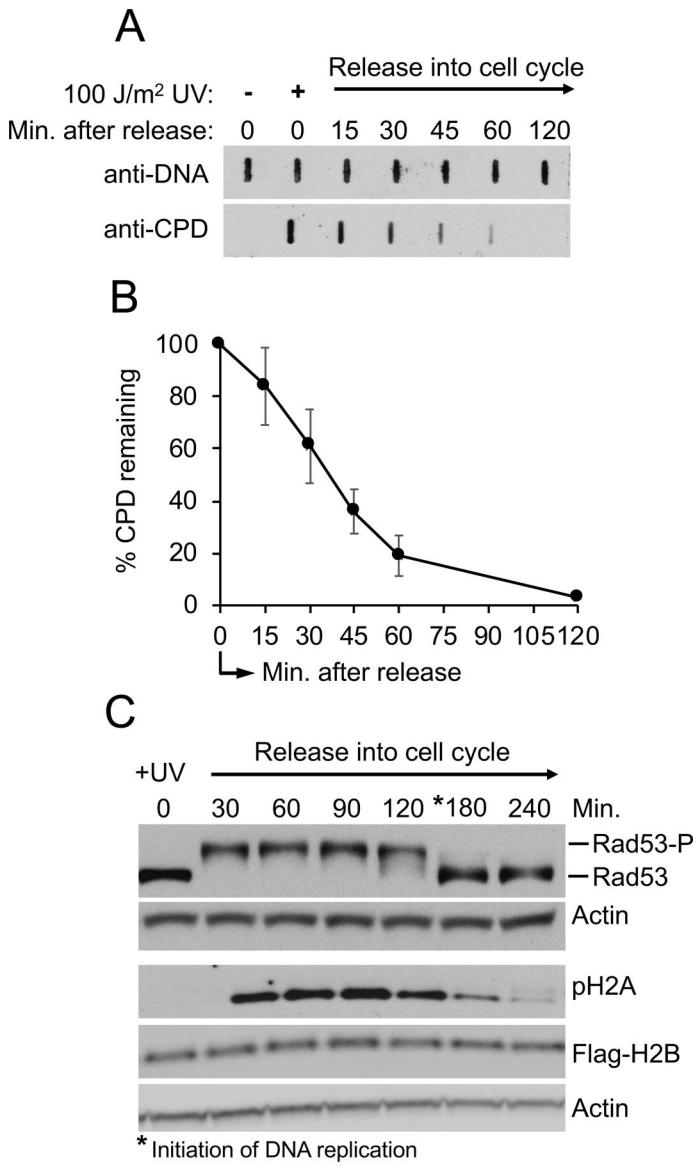

Figure 2. CPD lesions are formed and removed in quiescence cells after UV irradiation.

Quiescent cells were irradiated with 100 J/m^2 UVC and samples were collected at the time of irradiation and after release into YPD medium.

A. Levels of CPDs measured with anti-CPD antibody, with gDNA levels serving as loading control. A representative slot blot is shown.

B. Quantitation of CPD levels. The results represent the average of two independent experiments with standard deviation, and are relative to CPD levels formed at 0 min. C. DNA damage checkpoint. Western blot analysis using antibodies against Rad53 and phosphorylated H2A (pH2A).

*Time at which DNA synthesis was initiated. Flag-H2B and Actin represent loading controls.

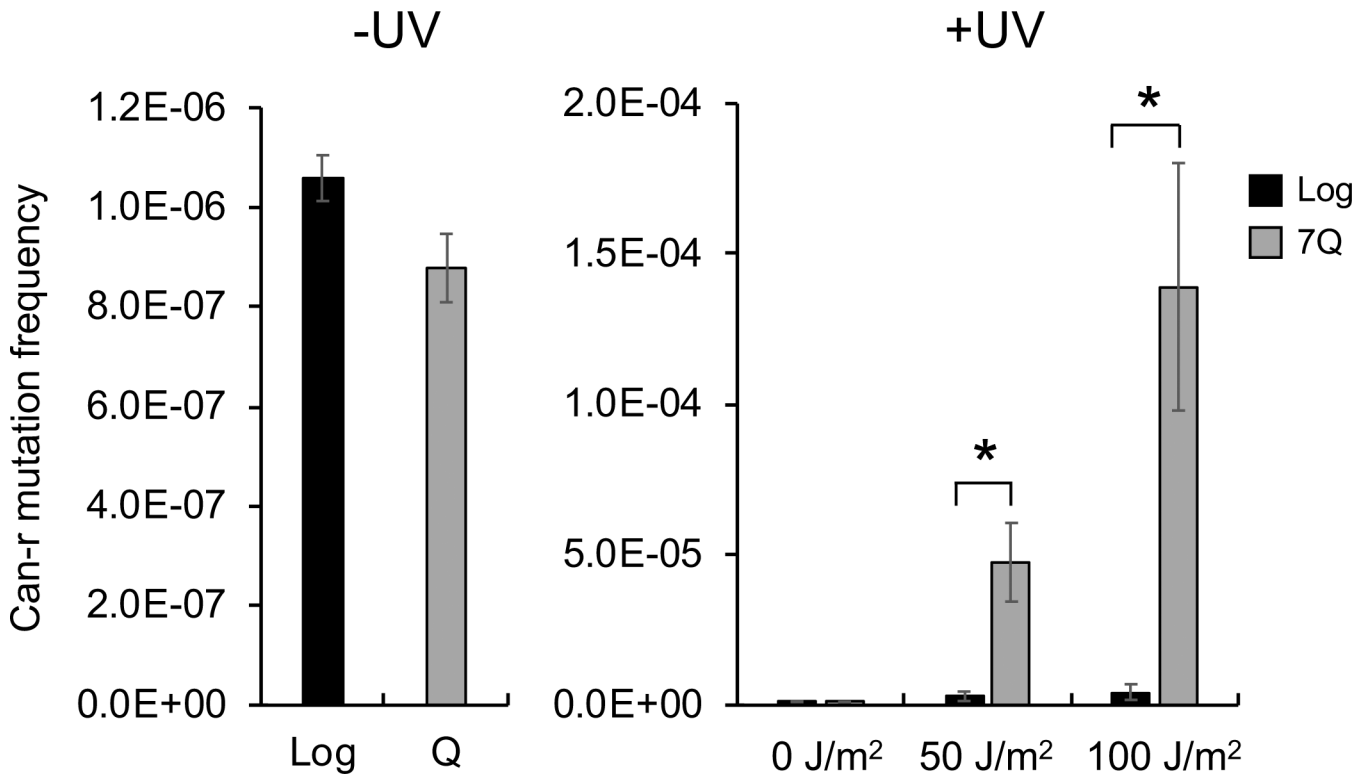

Figure 3. Q cells differentially express genes involved in NER and DNA synthesis.

Samples were collected from Log phase cells (Log), at 1-day intervals after inoculation (days 1–7), and from purified quiescent cells (7Q).

A. RT-qPCR analysis of RNAs isolated from Log or 7Q cells. The results represent the average of 3 independent experiments with standard deviation.

B. Detection of Rad7 (GGR-NER) and Rad26 (TCR-NER) using antibodies against HA-tagged proteins. * nonspecific band

C. Detection of replicative (Pol1, Pol2, Pol3) and translesion synthesis (Rev3, Rad30, Rev1) DNA polymerases using antibodies against Myc- or HA-tagged proteins.

Representative blots of Actin loading controls are shown.

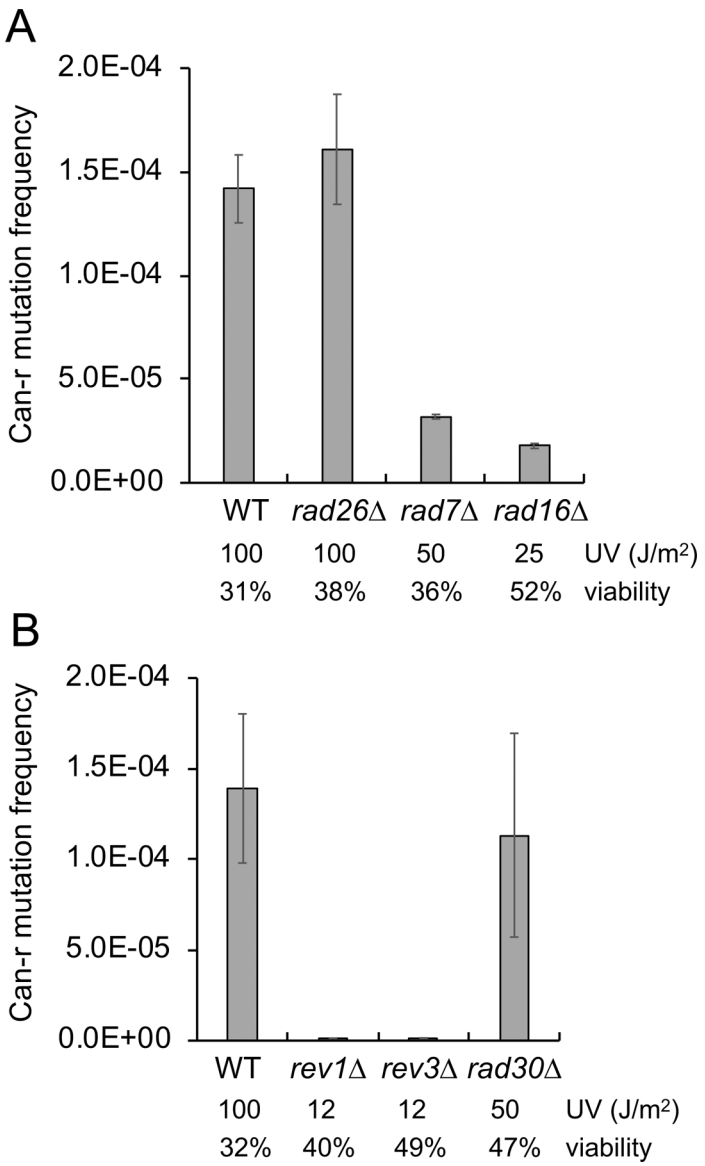

Figure 4. Quiescent cells have an increased frequency of UV-induced mutations.

Log phase and 7Q cells were unirradiated (−UV) or irradiated with 50 and 100 J/m^2 UVC (+UV) and plated in triplicate onto YPD plates containing canavanine. The results represent the average of 3–4 independent experiments with standard deviation. Asterisk represents a P value of <0.05 as determined by Student's T test.

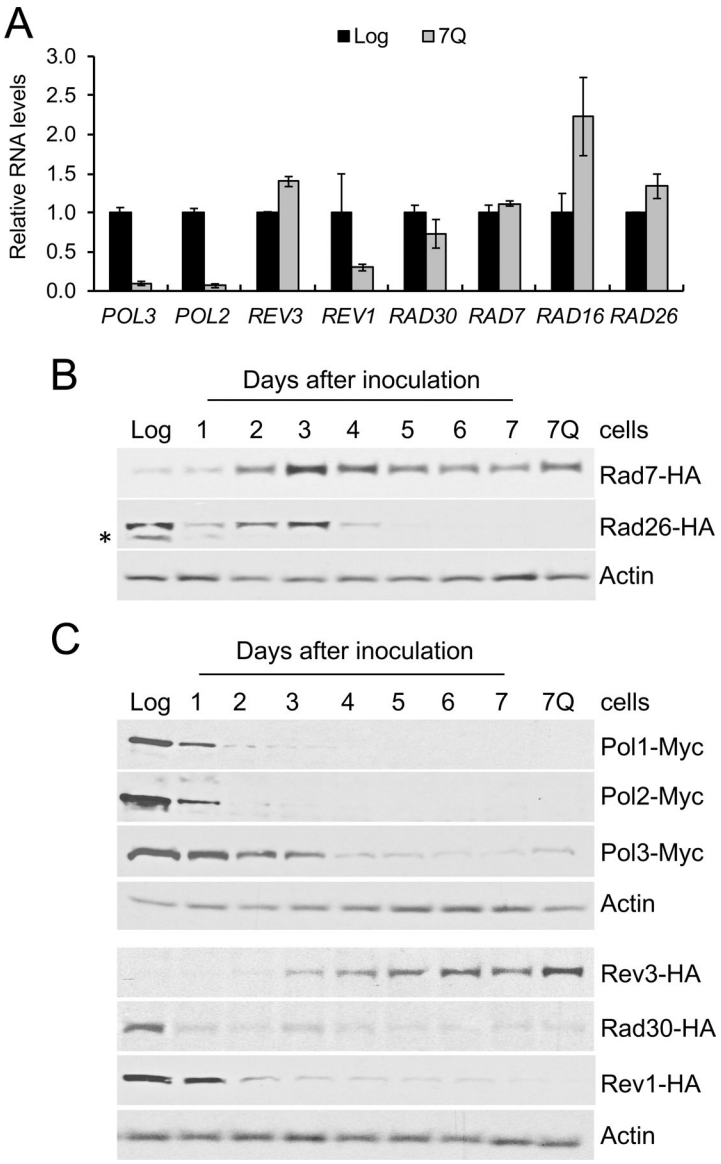

Figure 5. Frequency of UV induced mutations in quiescent cells defective in lesion recognition or in the absence of translesion synthesis DNA polymerases.

7Q wild type (WT) or mutant cells with deletion of genes required for (A) TCR-NER (*rad26Δ*), GGR-NER (*rad7Δ, rad 16*Δ), or (B) translesion DNA polymerase activity (*rev1*Δ, r*ev3*Δ, r*ad30*Δ) were exposed to doses of UV that resulted in equivalent levels of viability and plated in triplicate onto YPD plates containing canavanine. The results represent the average of 3–5 independent experiments with standard deviation.

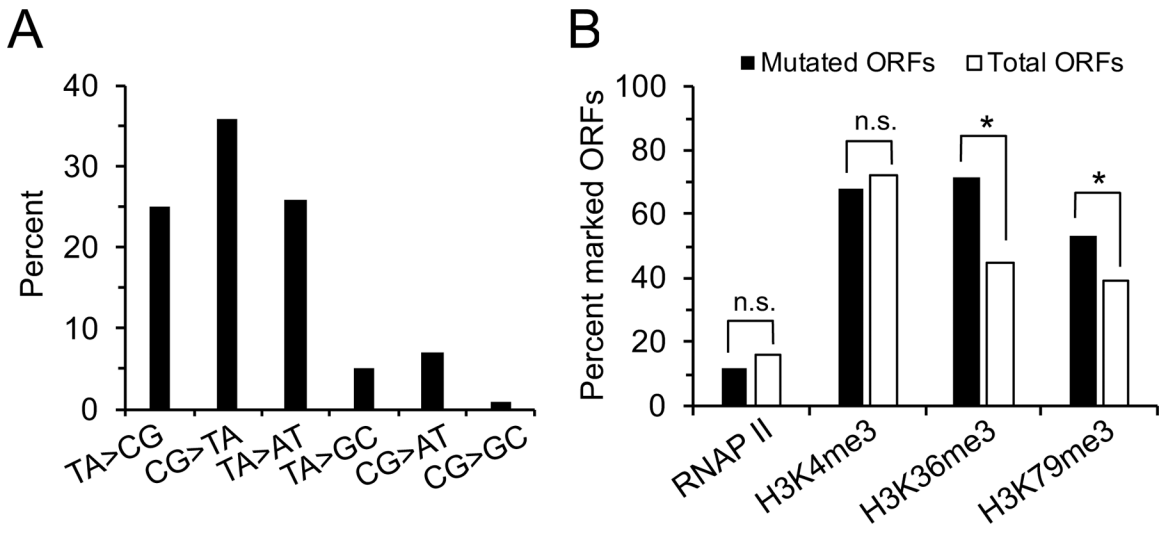

Figure 6. UV-induced mutational spectra in quiescent cells.

Three independent pools of 7Q cells were exposed to 100 J/m^2 UVC, and whole genome DNA sequencing was performed after growth of a Can-r colony arising from each pool.

A. Percentage of transition and transversion mutations (Table S4).

B. Percentage of mutated and total ORFs marked with RNA polymerase II (RNAPII), H3K4me3, H3K36me3 or H3K79me3 (Young *et al.*, 2017).

*p<0.05